

Responses to Reviewers' Comments for Manuscript

**The LOLland offshore Lidar EXperiment
(LOLLEX): A novel observational
approach for the study of wind farm flow
and entrainment**

Addressed Comments for Publication to
Atmospheric measurement techniques

by

Malekmohammadi et al.

1 Authors' Response to Reviewer 2

1.1 General comment

General Comments. Overall, the paper presents a broad overview of the LOLLEX campaign but fails to provide important details. The paper could be improved by incorporating an expanded joint analysis of the mean wind observations conducted with two lidars and the turbulence data from the vertical stares.

Response:

We would like to thank the reviewer for their thorough review. We acknowledge that the paper falls short of an in-depth joint comparison between the measurements of the two lidars and also the turbulence data for the entire campaign. We have attempted to include this analysis in the manuscript. In addition, we have carefully revised the manuscript based on the specific comments below. We hope that this new version addresses the comments of the reviewer.

1.2 Specific comments

Comment 1

In Fig. 4, it would be good to add the elevation angle for the DBS scan. Also, what was the motivation for using a 4-beam rather than 5-beam (with the 5th beam pointing vertical) DBS scan with the WindCube100s similar to the WindCubeV2 DBS scan? Please clarify if the WindCube100s DBS scans runs for 5-min how many estimates of u , v , w are retrieved, and if they are then averaged into 5-min samples.

Response:

Thank you for your comment, the figure is updated accordingly. After re-checking the instrument logs, we confirm that the WindCube 100S was configured to perform a 5-beam DBS scan rather than a 4-beam scan as initially stated. During each 5-minute DBS period, approximately 80 individual measurements were collected, which corresponds to an effective sampling rate of about 0.3 Hz. From

these measurements, instantaneous values of wind velocity and wind direction were retrieved; these were then averaged in post-processing to form 5-minute mean wind components.

We have updated figure 4 and added the following to the section 2.2.1:

In vertical stare mode, which corresponds to a line-of-sight (LOS) configuration with an elevation angle of $\varphi = 90^\circ$, the lidar operated at a sampling frequency of 1 Hz at ranges between 50 m and about 2500 m. In DBS mode, the lidar operated using a five-beam scanning configuration. Four oblique beams were sequentially emitted at an elevation angle of $\varphi = 75^\circ$ and azimuth angles of $\alpha = (0^\circ, 90^\circ, 180^\circ, 270^\circ)$, followed by a vertically pointing beam with an elevation angle of $\varphi = 90^\circ$ at ranges between 50 m and about 2500 m (Fig. 3). During each 5-min DBS period, approximately 80 individual samples were collected, corresponding to an effective sampling frequency of 0.3 Hz. In wind profiling mode, the lidar retrieves wind speed and wind direction. Both instantaneous estimates and 5-min time-averaged products were computed in post-processing (see Section 3.3).

Comment 2

The caption of Fig. 5 mentions a top and bottom panel, but the figure shows a left and right panel.

Response:

Thank you for the feedback. This oversight is now corrected.

Comment 3

The paper states: "When deployed on the vessel, the WindCube100S occasionally produced short or incomplete scans, likely due to its sensitivity to rapid translation and acceleration. Unlike the WindCubeV2, which is designed for dynamic conditions on buoys, the WindCube100S is not optimised for mobile offshore deployments. Despite these limitations, a large number of high-quality scans were obtained, providing valuable measurements within the wind farm. Outlier removal was accomplished by a moving median absolute deviation filter, following the recommendation by Starckenburg et al. (2016) and Leys et al. (2013)." For a campaign overview paper, it would be good to add quantitative information about the percentage of datasets flagged and removed.

Response:

We have revised the section 3.1:

The WindCube100S occasionally produced short or incomplete scans when deployed on the vessel, likely due to its sensitivity to rapid translation and acceleration. This can be attributed to its mechanically rotating scanning head for beam steering, in contrast to the WindCubeV2 Offshore, which operates without moving parts and is designed for dynamic buoy deployments. For the vertical scanning mode conducted between 2023-01-25 and 2023-08-28 (approximately 9,900 scans), 65% of the WindCube100S scans were flagged as incomplete (scan duration < 10 min) and excluded, while 30% achieved the full 25-min duration.[...]

Comment 4

The description of the filtering applied to the Halo lidar at the top of page 10 of the paper is not very clear - what motivated this particular method? Is the filtering done for each individual RHI scan or over a certain period? What is the percentage of data removed?

Response:

We have rephrased the corresponding paragraphs and refined the description of the data filtering as follows:

Following [Päschke et al. \(2015\)](#), a signal-to-noise ratio (SNR) threshold of -20 dB is commonly recommended for radial velocity data from the Halo Photonics Stream-Line XR+. In the present case, this threshold appeared overly conservative. The lidar data were used solely for mean wind speed estimation, and the beam was frequently oriented at angles close to 90° relative to the mean wind direction, resulting in generally low SNR values. In addition, the SNR was originally provided on a linear scale, with a substantial fraction of values being negative, preventing a consistent conversion to dB.

For the case study 4, a moderate correlation ($\rho \approx -0.63$) was found between the SNR and $|v_r - v_0|$, where v_r is the along-beam (radial) velocity and v_0 denotes the most probable radial velocity. However, substantial overlap between low- and high-deviation data across the SNR range indicates that SNR alone is not a reliable indicator of data quality. Consequently, no SNR-based filtering was applied. Radial velocity data were first filtered to remove implausible values by discarding samples with $|v_r| > 30 \text{ ms}^{-1}$. The most probable radial velocity v_0 was then estimated as the mode of the v_r distribution. Only samples satisfying $|v_r - v_0| < k \text{MoAD}$ were retained, where $\text{MoAD} = \text{median}(|v_r - v_0|)$ denotes the median absolute deviation about the modal radial velocity v_0 , and $k = 3$ is a dimensionless threshold parameter.

In summary, the filtering does not rely on SNR but instead on the statistical structure of the radial velocity distribution, which was found to be more robust for the present dataset due to the large number of undefined values (SNR < 0 in linear scale). The rationale for this approach is illustrated in Fig. 1, which shows the distribution of v_r , the estimated mode, and the retained interval. The filtering was applied independently to each RHI scan.

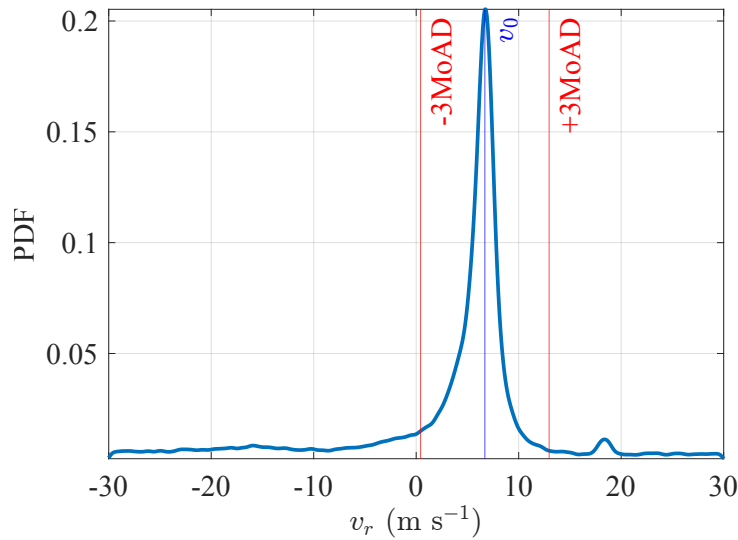


Figure 1: Probability density function of the along-beam velocity for the scanning lidar on the transformer platform (case study 4). The modal velocity v_0 is indicated, and the retained data correspond to the interval $|v_r - v_0| < 3 \text{MoAD}$.

Comment 5

The paper introduces the motion correction and states: "The efficacy of this algorithm has been validated under controlled conditions using a six-DOF motion platform (Malekmohammadi et al., 2024). Thus, this motion correction approach is well-suited for the deployment of DWLs on CTV or other vessels." In the cited paper, the algorithm was only validated for one test with pitch motion, the performance for other motions is not documented and it thus remains unclear how well it performs in a complicated ship-based deployment with different types of motions. No comparisons between uncorrected and corrected data are provided and it is unclear how critical the corrections are and if the corrected data look reasonable. In fact, I am not even sure they were applied in this paper.

Response:

We thank the reviewer for raising this important point. Motion correction was applied to the dataset used in the manuscript. To clarify its impact, we now explicitly include a comparison between uncorrected and corrected wind speeds in Section 5.1 Motion correction results.

During revision, and following comment 14, we carefully re-examined the motion correction algorithm and identified a bug in the translational motion correction, which led to an artificial increase in RMSE. In Malekmohammadi et al. (2024), rotational motion dominated and translational motion was limited. In the present campaign, however, the CTV's translational motion represents the primary source of motion-induced error, which helped to detect this issue.

After correcting the algorithm, we re-applied the motion correction to the entire dataset and compared the results against NORA3, which are presented in Section 5.1.

Comment 6

A tilt correction introduced in a previous publication by the lead author (Malekmohammadi et al., 2025) is discussed in section 3.3 but open questions remain. In one of the methods, the vertical component w from the WindCubeV2 is used as target to be matched when evaluating the tilt angle. Fig. 7 shows that the WindCubeV2 w -values at 150-m are non-zero (≈ 0.3 m/s) at the beginning of the time period plotted but then approach zero. How is it known that this trend in w is not caused by motions of the lidar but is in fact the true value that should be matched but the scanning lidar?

Response:

We thank the reviewer for raising this point. The decrease in \bar{w} is consistent with the evolution of the mean wind speed during that day. From the early hours toward the evening, the mean horizontal wind speed at 150 m (\bar{u}) decreased substantially, from approximately 20 m s^{-1} to about 5 m s^{-1} . If the flow has a small but approximately constant tilt angle α , the mean vertical velocity scales with the horizontal wind speed according to $\bar{w} \approx \bar{u} \tan(\alpha)$; thus \bar{w}/\bar{u} remains approximately constant while \bar{w} varies proportionally with \bar{u} . Consequently, a decrease in \bar{u} should lead to a corresponding decrease in the observed \bar{w} . This behaviour is consistent with Fig. 7, where \bar{w} is around 0.3 m s^{-1} when $\bar{u} > 15 \text{ m s}^{-1}$ and approaches zero as \bar{u} further decreases. While strong winds could in principle introduce small platform tilts even in harbour, the observed scaling of \bar{w} with \bar{u} is consistent with a tilted mean flow rather than an instrumental artifact.

To avoid focusing on a single day and to provide a more robust assessment of the static tilt correction algorithm, we removed the figure showing one day of data and

instead present the probability density function (PDF) of the vertical velocity difference between the WindCube100S and the WindCubeV2 using data collected between 2023-01-01 and 2023-07-12 (more than 6000 samples). This analysis demonstrates that the proposed static tilt correction performs well and outperforms both the non-corrected approach and a simple bias correction in which the bias is assumed to be the value of \bar{w} measured at height 400 m, far from ground obstacles.

Comment 7

Applying, the tilt correction to the WindCube100S shows strange results: in the afternoon the black line (scanning lidar) suddenly does not agree with the WindCubeV2 w -values (blue line) and no explanation is given about what is causing this sudden discrepancy.

Response:

We thank the reviewer for pointing this out. The discrepancy observed in the afternoon in the former Fig. 7 coincided with a short rain shower, as indicated by the CNR signal and the temporal pattern of w . Precipitation can occasionally introduce spurious vertical velocity signals in Doppler lidar measurements when falling hydrometeors contribute to the backscatter. In this case, the rain was not intense enough to cause data loss but likely led to artificially elevated w values for a short period. Since precipitation effects on Doppler lidar measurements are beyond the scope of this study and such events were rare in the dataset, we did not analyse them further. To avoid drawing conclusions from a single day, the figure has been removed and replaced with a probability density function (PDF) of the vertical velocity difference between the WindCube100S and the WindCubeV2 using data collected between 2023-01-01 and 2023-07-12. We also added a brief statement in the manuscript noting that precipitation can occasionally introduce spurious vertical velocity signals in Doppler lidar measurements and that such events were not specifically analyzed here.

Comment 8

Also, what tilt angle is determined when using the alternative method of forcing mean w at 400 m to be zero??

Response:

The alternative method does not explicitly determine a tilt angle. Instead, it assumes that the long-term mean vertical velocity at 400 m should be zero and removes any constant bias in w at that height. The removed offset is implicitly interpreted as the effect of a static tilt of the lidar. Thus, this approach applies a constant correction to the vertical velocity component rather than estimating a geometric tilt angle. Our analysis showed that this method tends to over-correct the data, particularly under conditions with non-zero large-scale vertical motion. For this reason, we developed and applied the revised approach described in [Malek-mohammadi et al. \(2025\)](#), which provides a more physical estimation of the static tilt effect.

Comment 9

If the tilt angle is known from visual inspections, why are any of the other methods needed?

Response:

The tilt angle inferred from installation photographs represented only the initial geometric alignment and did not account for quasi-static changes in vessel attitude during operation. The equilibrium attitude of the CTV can vary due to changes in mass distribution (e.g. fuel consumption or freshwater usage), producing a slowly varying static tilt. Such a tilt introduces a vertical velocity bias approximately given by

$$w_{\text{bias}} \approx \bar{U} \sin \theta.$$

Under high wind speed conditions (e.g. $\bar{U} \approx 20 \text{ m s}^{-1}$), even small tilt angles can therefore generate a great artificial vertical velocities.

Nonetheless, we have used a constant value of 2.7° for simplicity, since this could lead to greater data loss when DBS data from the 100S are unavailable. A more detailed analysis could assess how the tilt angle depends on the vessel's mass distribution (e.g., fuel, freshwater, and payload), but this is beyond the scope of the present study.

We have clarified this in the manuscript as:

The tilt angle derived from visual inspections represents the initial geometric alignment. During operation, quasi-static changes in vessel attitude (e.g. due

to varying mass distribution) may occur and introduce a vertical velocity bias of approximately $w_{\text{bias}} \approx \bar{U} \sin \theta$. In principle, the effective static tilt angle can be estimated for each measurement period using the Eq. 10. In this study, however, a constant value of 2.7° is used for simplicity and to preserve high data availability.

Comment 10

Finally, Fig. 7 shows data for one day. For a campaign overview paper, I would expect to see a more detailed statistical evaluation of the tilt correction with quantitative information about e.g. mean bias before and after the different corrections were applied.

Response:

We agree with the reviewer. To have a better picture, we have calculated the probability density function (PDF) of the Δw between the WindCube100S and the WindCubeV2 for the entire campaign and replaced figure 7 with fig. 2. We have also added the following to the main text:

Figure 2 presents the probability density function (PDF) of the vertical velocity difference between the WindCube100S and the WindCubeV2, using three different methods for tilt correction: no correction, a correction assuming $\bar{w} = 0$ at 400 m, and tilt correction with $\theta = 2.7$ derived from Eq. 10. The corrected WindCubeV2 is used as the reference instrument due to its dedicated wind-profiling configuration, continuous DBS operation, lower mechanical complexity, and consequently higher robustness and lower measurement uncertainty compared to the scanning WindCube100S. The PDF is computed from all available high-quality data collected between 2023-01-01 and 2023-07-12 (> 6000 samples). Without correction, the vertical velocity from the scanning lidar exhibits a positive bias, with a median of 0.28 m s^{-1} and values reaching up to 1 m s^{-1} . Applying a constant correction based on the assumption of zero mean vertical velocity at 400 m reduces the bias but over-corrects, resulting in a negative median of -0.20 m s^{-1} . The tilt-correction method based on Eq. 10 yields the lowest absolute bias (-0.05 m s^{-1}), the lowest root-mean-square error relative to the WindCubeV2, thus producing a noticeably narrower PDF, indicating improved accuracy and precision compared to the other approaches. It should be noted that in turbulence analysis, velocity components are decomposed into mean and fluctuating parts using Reynolds

decomposition

$$i = \bar{i} + i', \quad (1)$$

where $i = \{u, v, w\}$. The static tilt correction is therefore applied to obtain an unbiased estimate of the mean vertical velocity without assuming it to be zero. This correction does not affect the turbulence statistics, as these are computed from the fluctuating component, which by definition has zero mean. Hereinafter, the scanning lidar data are shown with tilt correction using Eq. 10.

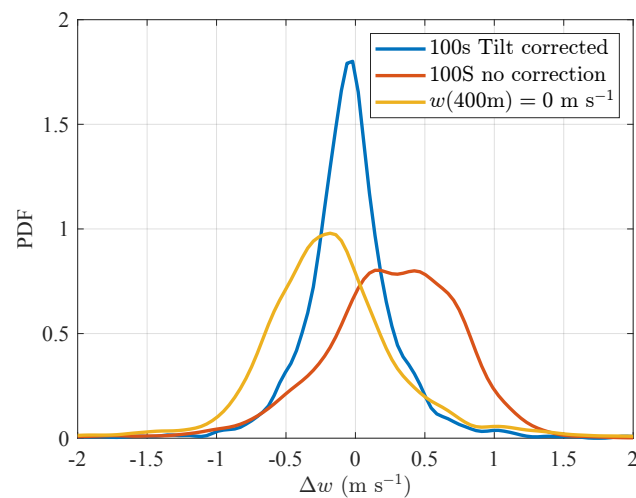


Figure 2: Probability density function (PDF) of the vertical velocity difference between the WindCube100S and the WindCubeV2 using data collected between 2023-01-01 and 2023-07-12 (> 6000 samples).

Comment 11

In line 269 it should say: “ Fig. 10 shows a comparison between the wind roses from WindcubeV2 and NORA 3 data.”

Response:

The line 269 was updated to

"[...] shows a comparison between the wind roses from NORA3 and WindcubeV2 data at 150 meters above sea level. "

Comment 12

The time series analysis in section 4.2 is confusing. I could not track down the source of Eq. 7 which is called an empirical fit to the Durst curve from 1960. Durst's work focused on relating maximum gust wind speeds to longer term mean wind speeds. Here the comparison deals with comparing hourly (but equivalent to 10min averages?) NORA 3 data to the Wind Cube 100s data (5-min averages recorded every 30 min) and Wind Cube V2 data (10-min averages). While I value the attention to the effect of different averaging times when comparing the data I do not see the value of blindly applying Eq. (7). The lidar scanning itself leads to averaging. Were the high-resolution time series of the Wind Cube V2 data and Wind Cube 100s not available for reprocessing using different averaging times? It would be best to compare 5-min vs. 10-min averages from the V2 and estimate if corrections should be applied to the 100s. The vertical resolution of the different lidars and the model data should also be discussed as it also affects the data. Also, Fig. 11 shows the temporal trends, but it is not ideal for visualizing the agreement or disagreement between the data sets. Scatter plots would be much better.

Response:

We agree that the effect of different averaging periods should be evaluated directly using the lidar measurements. Following this suggestion, we reprocessed the high-resolution lidar data and compared 5-min and 10-min averages derived from the WindCubeV2 measurements. The resulting differences in bias are small (within about 1%), indicating that the averaging-time difference has only a minor impact; therefore no correction was applied and Eq. (7) and the discussion related to the Durst curve were removed from the manuscript. To improve the comparison between datasets, we added scatter plots comparing the lidar measurements with the NORA3 data, in addition to the vertical profiles of bias and RMSE for the mean wind speed \bar{u} (with and without motion correction), which better illustrate the agreement between datasets. The WindCubeV2 and WindCube100S have comparable probe volume lengths (≈ 25 m); therefore, differences in vertical resolution are negligible.

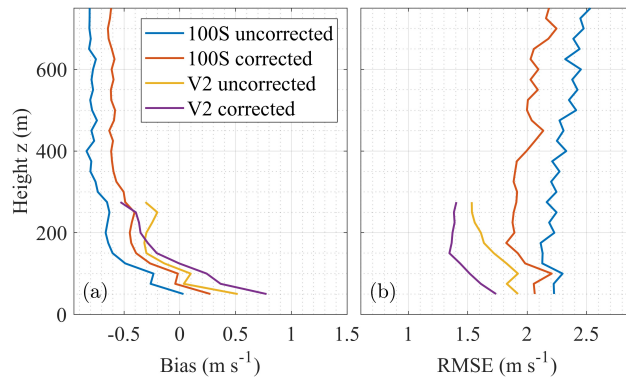


Figure 3: Comparison between the NORA3 and wind lidar measurements at various heights during the LOLLEX campaign. Left: Mean bias between NORA3 and the WindCube100S scanning lidar uncorrected (blue), corrected (red), WindCubeV2 lidar wind profiler uncorrected (orange), and corrected (purple), based on 10-minute averaged wind speed. Right: Root mean square error (RMSE) between NORA3 and the two lidars before and after motion correction.

Comment 13

In line 300, the reader should be pointed to Fig. 12

Response:

That is correct. The reader now is pointed to the appropriate figure.

Comment 14

In line 303 the authors write: “The RMSE is slightly higher for the WindCubeV2, which may be caused by uncertainties introduced during motion correction” Does this mean the motion correction makes things worse?

Response:

After correcting the motion-correction algorithm (see response to Comment 5), we recomputed the bias and RMSE profiles shown in Fig. 3. We have revised the manuscript accordingly.

Comment 15

In line 306 it is stated "Overall, both lidars show consistent performance compared to NORA3, especially above the rotor layer." How is consistent performance defined?

Response:

We acknowledge that the term "consistent performance" was used ambiguously and have therefore removed this statement from the manuscript.

Comment 16

Lines 324-238: "Before the event, a bright and persistent CNR maximum around 600 m indicates aerosol accumulation beneath the capping inversion, a common precursor to shear-driven instabilities." What causes the aerosol accumulation and what exactly serves as precursor to shear-driven instabilities?

Response:

We thank the reviewer for pointing out the ambiguity in our original formulation. We have removed the "*precursor to shear-driven instabilities*" phrasing, which may have caused confusion and we have revised the manuscript for clarification as

A bright and persistent CNR maximum is observed near 600 m (Fig. 12). This maximum corresponds to aerosol accumulation beneath the capping inversion at the top of the stable boundary layer. Strong temperature inversions can suppress vertical turbulent mixing and limit dispersion, leading to the accumulation of aerosols below the inversion (Zhang et al., 2024). Vertical wind shear due to the change from typical sub-geostrophic wind speeds in the ABL towards geostrophic winds in the free atmosphere above can create favourable conditions for Kelvin-Helmholtz instabilities.

Comment 17

The uncertainties discussed in line 338-343 are critical for DBS or VAD lidar scans, but the results shown are from the vertical stares.

Response:

Thank you for raising this point. We have removed this paragraph.

Comment 18

Did the Wind Cube V2 measurements add any value to the analysis of the KHB?

Response:

We thank the reviewer for this question. In the KHB case study, the billows occurred above the maximum measurement range of the WindCubeV2, so this instrument was not used to directly observe the billow structures. However, the WindCubeV2 measurements were used to provide independent wind speed profiles in the lowest part of the marine atmospheric boundary layer (below about 300 m), which helped increase confidence in the mean wind speed profiles derived from the scanning lidar and used in the analysis of the case study.

Comment 19

Fig. 14 only shows results from the vertical stares with the 100s, but the discussion in section 5.2 also mentions wind speed and negative wind speed gradients. Where are those shown? Why are the data from the two lidar systems and different scans with the 100s not analyzed together?

Response:

We appreciate for pointing out this oversight. Now we have added profiles of the mean wind speed recorded by the WindCube V2 and the WindCube100S and NORA3 in manuscript (see Figure 4).

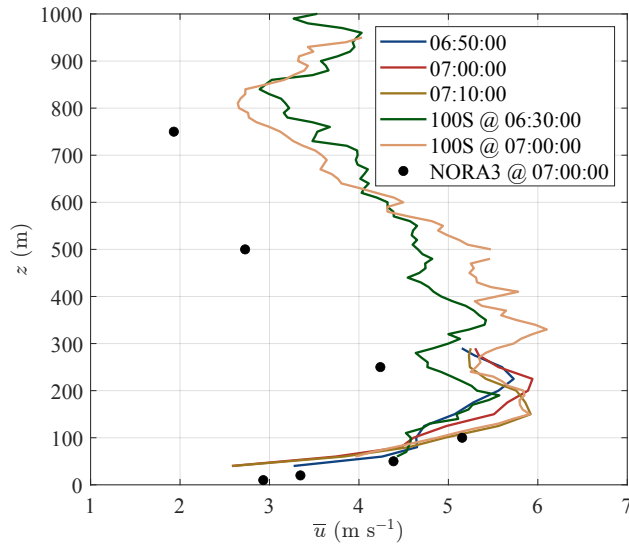


Figure 4: Profiles of the mean wind speed recorded by the WindCube V2 and the WindCube100S on 22 February 2023 between 06:30 and 07:10 in the harbour.

Comment 20

Near line 380 in this text: "Between 06:47 and 07:00, $I_w \approx 0.05$ at 500 m and between 07:05 and 07:12, the turbulence intensity has nearly doubled with $I_w \approx 0.09$ at 500 m. It should be noted that the lidar beam spatial averaging leads to an underestimation of the turbulence intensity I_w by 20-30%." How is I_w computed given the different sampling times of w and u ? How was the underestimation of 20-30% determined?

Response:

We thank the reviewer for raising this point. In the revised manuscript, we no longer use the turbulence intensity I_w and instead analyse the variance of w directly. This avoids the need to combine w measurements from the vertical staring mode with wind speed profiles obtained from the DBS scans and therefore removes the need for temporal interpolation between the two datasets. To better quantify turbulence and its dependency on the time, we added power spectral density (PSD) estimates of the vertical velocity before and after the observed increase in turbulence. The low-pass filtering, i.e., the along-beam spatial averaging, is always present but becomes more apparent when turbulence fluctuations increase. This is because the signal-to-noise ratio also increases with wind speed, thus the

high-frequency measurement noise that dominates at low wind speeds becomes less visible.

Comment 21

In line 396 a skewness profile is mentioned, where is this shown?

Response:

We have added the following text and figure to the manuscript:

The moving standard deviation of σ_w (Fig. 13 c) and the profile of σ_w (Fig. 5 a) show both a local increase of the vertical turbulent fluctuations at heights between 200 and 800 m above the surface. Figure 5 also presents the vertical profiles of kurtosis (b) and skewness (c) for three observational windows (06:35-06:47, 06:47-07:00, and 07:05-07:12), together with the corresponding power spectral densities of w at 430 m. Prior to 06:47, σ_w is relatively uniform between 100 and 800 m, with weak turbulence ($\sigma_w < 0.2 \text{ m s}^{-1}$) between 100 and 700 m above ground level. During this period, the power spectral density S_w exhibits pronounced white noise at frequencies above 0.1 Hz, indicating that turbulence fluctuations are too weak to be reliably resolved by the instrument. From 06:47 onwards, σ_w increases locally near 600 m and subsequently reaches values of approximately 0.5 m s^{-1} between 400 and 600 m. Between 06:47 and 07:00, the S_w spectra indicate improved detectability of turbulent fluctuations, although noise levels remain sufficiently high to partially obscure the effects of along-beam spatial averaging. After 07:05, vertical velocity fluctuations peak near 430 m, and the corresponding S_w spectrum shows reduced noise levels, with along-beam spatial averaging associated with the lidar probe-volume length becoming apparent at frequencies above 0.1 Hz, where the spectral slope steepens relative to the $-5/3$ inertial subrange. The pronounced spatial and temporal variability of σ_w reflects a non-stationary and vertically evolving boundary layer, suggesting the onset of downward transport from the boundary-layer top.

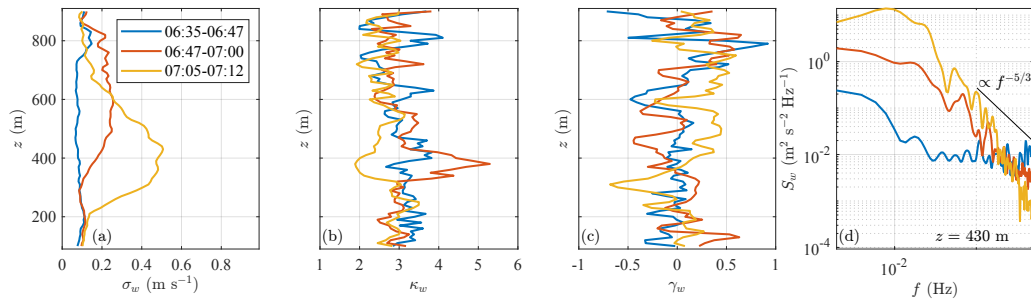


Figure 5: Profiles of the standard deviation σ_w (a), kurtosis κ_w (b), skewness γ_w of the vertical velocity component w (c), and the power spectral density of S_w at 430 m (d). All panels are based on data recorded by the WindCube100S in the harbour on 22 February 2023 between 06:35 and 07:16.

Comment 22

In case study 3 (section 5.3) the measurement location is not described and the data showing the low-level jet are not presented. This is a good example where the paper could be improved by presenting both the u and w observations together.

Response:

We have clarified this as

Case study 3 addresses observations of internal waves conducted in the harbour after the CTV returned from the offshore wind farm [...]

In addition, we have added the vertical profile of mean wind speed (fig. 6 a). This figure shows a low-level jet with its maximum at approximately 400 m. The profile is consistent between both lidars.

Comment 23

How do the spectra in Fig.16 compare to spectra for time periods prior/after the waves?

Response:

We thank the reviewer for this suggestion. To clarify this point, we added spectra for a period prior to the occurrence of the waves (22:05–22:15) and for a later

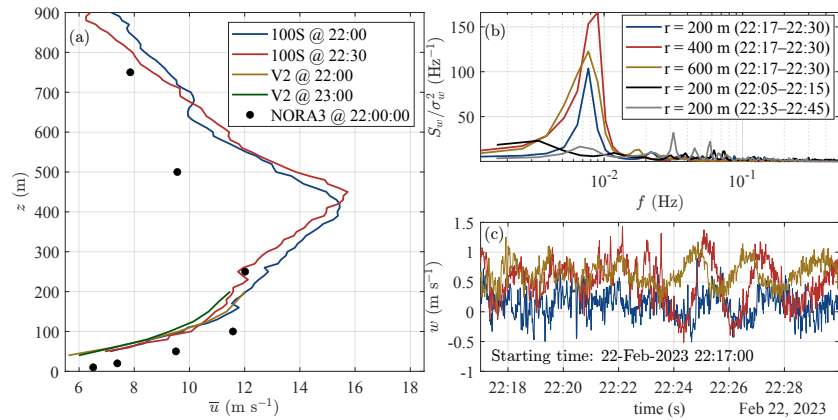


Figure 6: Panel (a): profiles of the mean wind speed measured by the WindCubeV2 and the WindCube100S on 22 February 2023 between 22:00 and 22:35 in the harbour. Panel (b): power spectral densities of the vertical velocity fluctuations from 200 to 600 m above the surface during the wave event (22:17–22:30). The black (grey) solid line shows the power spectral density at 200 m prior (after) to the observation of the waves for comparison. Panel (c): Time series of vertical velocity corresponding to the PSD shown in panel (b) between 22:17 and 22:30.

period (22:35–22:45) at 200 m in fig. 6 b. Before the waves appear, the power spectral density of the vertical velocity shows no distinct spectral peak, indicating the absence of wave activity at both 200 m and 400 m. After the waves develop, the spectrum at 200 m also does not exhibit a pronounced peak, consistent with the time series and suggesting that the wave signal does not extend down to this level. However, clear spectral peaks remain visible between approximately 350 and 600 m during the wave event, indicating that the wave activity is confined to higher altitudes near the nose of the low-level jet. These spectra have been added to Fig. 16 and described in the revised manuscript to clarify the vertical extent and temporal evolution of the wave signal.

Comment 24

Line 441-447: Could NORA 3 data not aid in the stability analysis for this case?

Response:

NORA3 could in principle be used to estimate atmospheric stability, for example through the Bulk Richardson number, as done in [Malekmohammadi et al. \(2025\)](#). However, its temporal and spatial resolution is limited relative to the scales of the processes investigated here. A more robust assessment would require co-located measurements with higher temporal and vertical resolution, such as temperature and humidity profiles from additional instrumentation, which were not available during the campaign. We have therefore not applied this approach and instead added the following sentence to the manuscript:

Moreover, although reanalysis products such as NORA3 could be used to estimate atmospheric stability (e.g., via the Bulk Richardson number), their temporal and spatial resolution is limited compared with the scales of the observed processes. A more robust assessment would require co-located, high-resolution profile measurements of temperature and humidity, e.g. by a passive microwave radiometer ([Westwater et al., 2004](#); [Rose et al., 2005](#)), a Raman lidar ([Lange et al., 2019](#); [Wulfmeyer & Behrendt, 2021](#)), or an infrared temperature profiler ([Knuteson et al., 2004](#); [Michaud-Belleau et al., 2025](#)). To obtain such measurements, a HATPRO RG4 profiler was installed at Rødsand harbour at the beginning of the campaign. Unfortunately, the instrument was malfunctioning, and no usable data could be obtained.

Comment 25

In section 5.4 details are missing about PY Wake (Ref?) simulations and the simulations mentioned in lines 465-467. The model performance should be expanded to provide quantitative information about model performance.

Response:

We have re-written section 5.4 entirely with a more focused study case combining the lidar V2 data and the data from the scanning lidar on the transformer platform and appropriate reference to PyWake ([Pedersen et al., 2023](#)).

Comment 26

Line 505: how was it determined that the V2 showed robust performance?

Response:

We thank the reviewer for this comment.

We have revised line 505 as:

The WindCubeV2 maintained considerably higher data availability during the campaign compared to the WindCube100S (by a factor of about 3.5). The WindCube100S showed a higher rate of scan interruptions, which we attribute not only to its mechanical configuration, specifically the relatively heavy two-axis external scanner head used to adjust both azimuth and elevation angles, but also to its sensitivity to platform motion. In particular, translational motions of the vessel appear to contribute to data loss and incomplete scans. In contrast, the WindCubeV2 uses optical switching without moving parts for beam steering (?), making it more robust under dynamic conditions. For the vertical staring mode conducted between 2023-01-25 and 2023-08-28 (approximately 9900 scans), 65% of the WindCube100S scans were flagged as incomplete (scan duration < 10 min) and excluded, while only 30% reached the full 25-min duration.

Comment 27

Line 508: how many data sets of the 100s are of good quality?

Response:

We have added the following to the line 508:

For the vertical staring mode conducted between 2023-01-25 and 2023-08-28 (approximately 9900 scans), 65 % of the WindCube 100S scans were flagged as incomplete (scan duration < 10 min) and excluded, while 30 % of the scans had a full 25-min duration.

References

Knuteson, R. O., Revercomb, H. E., Best, F. A., Ciganovich, N. C., Dedecker, R. G., Dirks, T. P., Ellington, S. C., Feltz, W. F., Garcia, R. K., Howell, H. B., Smith, W. L., Short, J. F., & Tobin, D. C. (2004). Atmospheric emitted radiance interferometer. part i: Instrument design. *Journal of Atmospheric and Oceanic Technology*, 21, 1763 – 1776. doi:[10.1175/JTECH-1662.1](https://doi.org/10.1175/JTECH-1662.1).

- Lange, D., Behrendt, A., & Wulfmeyer, V. (2019). Compact operational tropospheric water vapor and temperature raman lidar with turbulence resolution. *Geophysical Research Letters*, *46*, 14844–14853. doi:[10.1029/2019GL085774](https://doi.org/10.1029/2019GL085774).
- Malekmohammadi, S., Cheynet, E., & Reuder, J. (2025). Observation of Kelvin–Helmholtz billows in the marine atmospheric boundary layer by a ship-borne Doppler wind lidar. *Scientific Reports*, *15*, 5245.
- Malekmohammadi, S., Duscha, C., Jenkins, A. D., Kelberlau, F., Gottschall, J., & Reuder, J. (2024). Evaluating the performance of pulsed and continuous-wave lidar wind profilers with a controlled motion experiment. *Remote Sensing*, *16*, 3191.
- Michaud-Belleau, V., Gaudreau, M., Lacoursière, J., Boisvert, E., Ravelomanantsoa, L., Turner, D. D., & Rochette, L. (2025). The atmospheric sounder spectrometer by infrared spectral technology (assist): instrument design and signal processing. *Atmospheric Measurement Techniques*, *18*, 3585–3609. doi:[10.5194/amt-18-3585-2025](https://doi.org/10.5194/amt-18-3585-2025).
- Päschke, E., Leinweber, R., & Lehmann, V. (2015). An assessment of the performance of a 1.5 μ m doppler lidar for operational vertical wind profiling based on a 1-year trial. *Atmospheric Measurement Techniques*, *8*, 2251–2266.
- Pedersen, M. M., Forsting, A. M., van der Laan, P., Riva, R., Romàn, L. A. A., Risco, J. C., Friis-Møller, M., Quick, J., Christiansen, J. P. S., Rodrigues, R. V., Olsen, B. T., & Réthoré, P.-E. (2023). Pywake 2.5.0: An open-source wind farm simulation tool. URL: <https://gitlab.windenergy.dtu.dk/TOPFARM/PyWake>.
- Rose, T., Crewell, S., Löhnert, U., & Simmer, C. (2005). A network suitable microwave radiometer for operational monitoring of the cloudy atmosphere. *Atmospheric Research*, *75*, 183–200. doi:<https://doi.org/10.1016/j.atmosres.2004.12.005>. CLIWA-NET: Observation and Modelling of Liquid Water Clouds.
- Westwater, E., Crewell, S., & Mätzler, C. (2004). A review of surface-based microwave and millimeter-wave radiometric remote sensing of the troposphere. *URSI Radio Science Bulletin*, *2004*, 59–80. doi:[10.23919/URSIRSB.2004.7909438](https://doi.org/10.23919/URSIRSB.2004.7909438).

- Wulfmeyer, V., & Behrendt, A. (2021). Raman lidar for water vapor and temperature profiling. In T. Foken (Ed.), *Springer Handbook of Atmospheric Measurements* (pp. 719–739). Cham: Springer International Publishing. doi:[10.1007/978-3-030-52171-4_25](https://doi.org/10.1007/978-3-030-52171-4_25).
- Zhang, M., Tian, P., Zhao, Y., Song, X., Liang, J., Li, J., Zhang, Z., Guan, X., Cao, X., Ren, Y. et al. (2024). Impact of aerosol-boundary layer interactions on PM_{2.5} pollution during cold air pool events in a semi-arid urban basin. *Science of the Total Environment*, 922, 171225.